Optimal control of interior permanent magnet synchronous integrated starter-generator

L. CHÉDOT[1 2]
[1] Valeo Electrical System
2, rue A. Boulle / BP 150
94017 Créteil Cedex / France
Email: laurent.chedot@utc.fr

G. FRIEDRICH[2]
[2] Université de Technologie de Compiègne
Laboratoire d'Electromécanique / BP20529
60205 Compiègne Cedex / France
Email: guy.friedrich@utc.fr
Tel: 33 (0)3 44 23 45 15
URL: www.utc.fr/lec

Keywords

Permanent magnet motors, automotive applications, drives for HEV, adjustable speed drives, flux model.

Abstract

This paper deals with the optimal control of interior permanent magnet synchronous machine (IPM) in the integrated starter-generator (ISG) application. IPM designed for flux-weakening operations are able to realise high performances. Nevertheless, the ISG environment imposes lots of constraints which must be taken into account in an appropriate control. After a presentation of machine design, ISG constraints and control structure, models of the IPM and its environment are detailed including electromechanical calculations. An optimal control (total losses minimisation) based on a numerical, non linear constrained optimisation routine is described. Efficiencies in torque vs. speed plan point out the importance of taking into account voltage and power limitations against the operating range. The presented simulation results shows that Interior Permanent Magnet machine (IPM) is a good solution for ISG applications.

1 Introduction

The study of ISG application leads to make comparisons between different machines structures: induction machine, wound rotor synchronous machine, reluctant and permanent magnet machine [1–6]. All these machines must respect very strong rules and specifications (low size, high torque, speed and efficiency). In this context, IPM structure owns lots of advantages: high specific power, brushless, no losses in the rotor. IPM particularities, associated to ISG constraints (wide speed range, battery supply and highly variable temperature) impose a precise control.
After a presentation of machine design, ISG constraints and control structure, models of the IPM and its environment will be detailed including electromechanical calculations. Then, optimisation procedure will be established.

2 Machine and control structure

2.1 Design

Figure 1 shows a cross-section of a classical IPM adapted to flux-weakening operation [7, 8].

This structure cumulates the characteristics of permanent-magnet and reluctant machines [9]: torque is a combination of hybrid and reluctant torque; the induce voltage, due to the presence of permanent-magnet excitation, is constant and must be reduced by flux-weakening at high speed. Electrical and mechanical behaviour will be detailed in section 3.

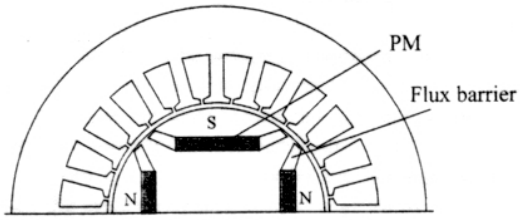

Figure 1: IPM cross-section [7]

2.2 Constraints due to starter-generator application

Starter-generator, as others automotive applications, is very constrained:

- low size;
- high torque at low speed with minimum power taken on the battery ($140\ Nm$ at $600\ A_{rms}$, $8\ kW$);
- operating points at high speed ($\rightarrow 6000\ rpm$);
- power and voltage limited by battery: $8kW$, 21 to 36 V in Motor mode (starter or boost) and 42 to 50V in Generator mode (power depending on battery technology);
- limited battery energy storage;
- current limited by inverter or thermic conditions ($150 \rightarrow 600\ A_{rms}$);
- high temperature variation ($25^oC \rightarrow 180^oC$).

These constraints create specific behaviours (high magnetic saturation) and limitations (current, voltage, power, energy). Moreover, terminal voltage, equal to the battery voltage, varies with the state of charge and the consumed power [10].

2.3 Control scheme

This machine is used as starter and generator. Its control is unified by using of unique torque control, positive torque for motor operations and negative torque for generator. Figure 2 shows this control scheme.

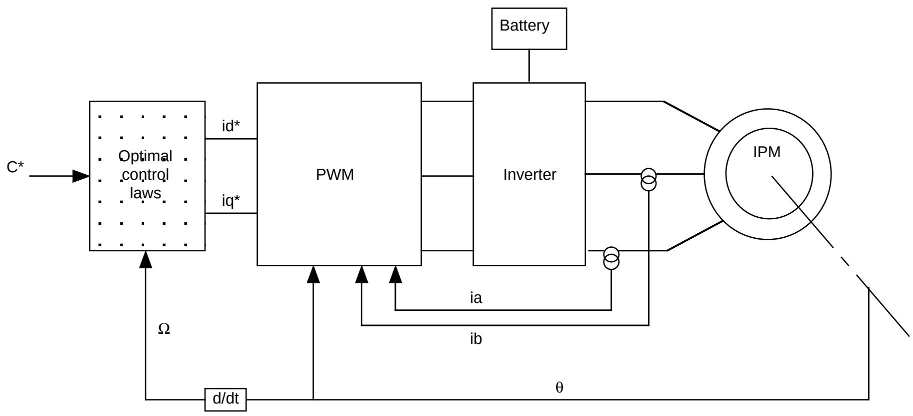

Figure 2: Optimal torque control

The optimal control laws, including flux-weakening [11, 12], can be explained thanks to circle diagram and the three control modes introduced by MORIMOTO and all. in [13]. In order to use simple analytical expression, a lot of hypotheses must be done: no magnetic saturation, constant terminal voltage, no temperature variation.

We show that, in the starter-generator application, these hypotheses can not be maintained. In these conditions, to realise a precise control including high efficiency, it become necessary to take into account all the non-linearities (machine and application) in a specific control.

One way is to compute, by numerical calculations, MORIMOTO's ideal trajectories with precise models of the machine.

3 Models

3.1 Machine

The IPM is modelled by classical Park's equations [14] (d-q reference frame) except for flux and iron power losses.

3.1.1 Saturation

Because of magnetic saturation, flux can not be expressed as functions of inductances. In each axe, the inductance saturates with the current (classical saturation) and moreover each current has an action on the others inductances (cross saturation).
Nevertheless, in the Park's equation, the relations linking flux with voltage and torque don't need hypotheses on magnetic saturation (Cf. equations 10, 13 and 14). These relations stay true in high magnetic saturation conditions.

Each flux ψ_d and ψ_q can be a non-linear function of the currents i_d and i_q.

$$\psi_d = f_d(i_d, i_q) \quad (1)$$
$$\psi_q = f_q(i_d, i_q) \quad (2)$$

f_d and f_q are calculated by interpolation of measures tables (Cf. figure 3) realised with the finite element (FE) software FLUX2D [15].

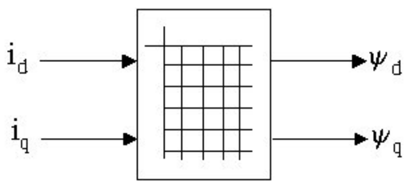

Figure 3: Flux table

For different operating points (i_d, i_q), and in presence of the permanent magnets, the 3 phase flux (ψ_a, ψ_b, ψ_c) are evaluated (internal function) and so, direct and quadrature flux are deduced:

$$\begin{pmatrix} i_d \\ i_q \end{pmatrix} \rightarrow Park^{-1} \rightarrow \begin{pmatrix} i_a \\ i_b \\ i_c \end{pmatrix} \rightarrow$$

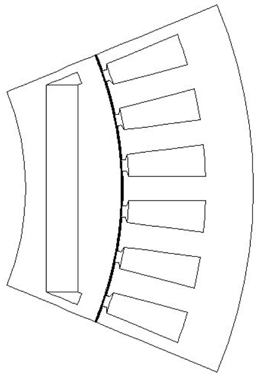

which give after resolution:

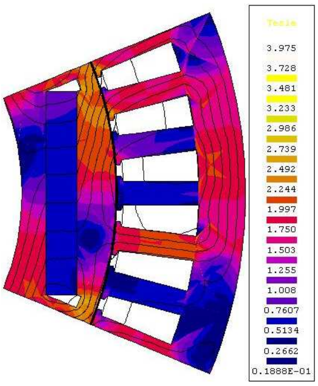

$$\rightarrow \begin{pmatrix} \psi_a \\ \psi_b \\ \psi_c \end{pmatrix} \rightarrow Park \rightarrow \begin{pmatrix} \psi_d \\ \psi_q \end{pmatrix}$$

3.1.2 Iron losses

Iron losses evaluation follows the same procedure, FE measurements (FLUX2D) for different speed and different operating points give tables of data which are interpolated

$$P_{iron} = f(i_d, i_q, \omega_s) \tag{3}$$

After the prototype construction, iron losses will be measured and the characteristics will be used for the optimisation.

3.2 Inverter

Inverter behaviour is considered as ideal. Its global efficiency and load voltage drop can be added easily.

3.3 Battery

Battery is modelled by a voltage source in series with an internal resistance as shown on figure 4. Maximum power supply is equal to:

$$P_{bmax} = \frac{E_b^2}{4R_b} \tag{4}$$

In generator mode, terminal voltage is regulated at a constant value (around). Battery is so modelled by a simple voltage source V_{ch}.

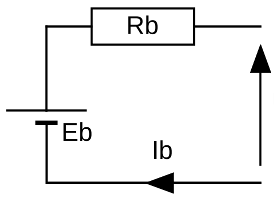

Figure 4: Battery electrical model

3.4 Electromechanical equations

For a given operating point (i_d, i_q and ω_s), all electrical and mechanical data are performed:

- current (RMS),

$$I_{rms} = \sqrt{\frac{i_d^2 + i_q^2}{3}} \tag{5}$$

- flux (table),

$$\psi_d = \psi_d(i_d, i_q) \tag{6}$$
$$\psi_q = \psi_q(i_d, i_q) \tag{7}$$

- iron (table) and total losses,

$$P_{iron} = P_{iron}(i_d, i_q, \omega_s) \tag{8}$$
$$P_{losses} = P_{iron} + 3R_s I_{rms}^2 \tag{9}$$

- electromagnetic, losses and mechanical torque,

$$T_{em} = p\left[\psi_d i_q - \psi_q i_d\right] \tag{10}$$
$$T_{iron} = \frac{P_{iron}}{\Omega} \tag{11}$$
$$T_m = T_{em} - T_{iron} \tag{12}$$

- voltage,

$$v_d = R_s i_d - \omega_s \psi_q \tag{13}$$
$$v_q = R_s i_q + \omega_s \psi_d \tag{14}$$
$$V_{rms} = \sqrt{\frac{v_d^2 + v_q^2}{3}} \tag{15}$$

- electrical and mechanical power,

$$P_e = v_d i_d + v_q i_q \tag{16}$$
$$P_m = T_m \Omega \tag{17}$$

- efficiency,

$$\eta = \left(\frac{P_m}{P_e}\right)^{sign(T_m)} \tag{18}$$

- battery voltage,

$$U_b = \frac{E_b + \sqrt{E_b^2 - 4R_b P_b}}{2} \tag{19}$$

  where P_b is the power given by the battery. It is equal to the electrical power divided by the inverter efficiency. If voltage are considered as sinusoidal, across voltage supply is equal to:

$$V_{sup} = \frac{U_b}{2\sqrt{2}} \tag{20}$$

- The maximum injectable current is equal to the maximum inverter current in starter mode and is limited by the maximum current density in the IPM in generator mode:

$$I_{lim} = \begin{cases} I_{inverter\ max} & (starter) \\ \propto J_{s\ max} & (generator) \end{cases} \tag{21}$$

4 Optimisation procedure

4.1 Principle

Controlling the IPM is equivalent to injecting the currents i_d, i_q which minimise the total losses with respect to different constraints (torque, current, voltage and power).

$$\forall(T^*, \Omega), \quad (i_d^*, i_q^*) \setminus \min_{i_d^*, i_q^*} \sum P_{losses}$$

with

$$\begin{aligned} T_m &= T^* \\ V_{rms} &\leq V_{disp} \\ I_{rms} &\leq I_{lim} \\ P_e &\leq P_{bmax} \end{aligned}$$

The MATLAB optimisation toolbox [16] provides a non-linear constrained optimisation routine. It minimise an *objective function* f and try to maintain *constrained functions* g negative:

$$x^* \quad \setminus \quad \min_{x^*} f(x^*)$$

with

$$g_i(x^*) \ < \ 0, \quad \forall i \ = \ 1..N_{constraints}$$

4.2 Objective function

The objective function is here the total losses (Cf. equation 9):

$$f \ = \ P_{losses} \tag{22}$$

4.3 Constraints functions

The constraints functions are:

- Mechanical torque (Cf. equation 12) is equal to the order torque:

  $$g_t = |T_m - T^*| - \epsilon |T^*| \tag{23}$$

  ϵ is a percentage ($0 < \epsilon < 1$) which defines precision.

- Current (Cf. equation 5) is less than the limit (Cf. equation 21):

  $$g_i = I_{rms} - I_{lim} \tag{24}$$

- across voltage (Cf. equation 15) is less than the available voltage (Cf. equation 20)

  $$g_v = V_{rms} - V_{sup} \tag{25}$$

- In starter mode, electrical power (Cf. equation 16) is limited by the battery maximum power (Cf. equation 4):

  $$g_p = P_e - P_{bmax} \tag{26}$$

4.4 Algorithm

1. The operating range is established. Speed is due to the application: from 0 to the application maximum speed ($5000\ rpm$). Maximum and minimum torques are calculated at standstill by a first constrained optimisation.

2. For each couple (T^*, Ω), $(i_d^*, i_q^*$ are calculated by optimisation as seen before.

5 Application

As an application, the currents are calculated and used to evaluate the IPM performances and operating range.

5.1 Environmental data

The previous calculation procedure is done with the following data and limits:

- temperature is close to the ambient temperature ($T = 25^oC$), stator resistance is so equal to: $R_s = 6.1\ m\Omega$;
- in starter mode, current is limited by inverter: $I_{lim} = 600\ A_{rms}$; and voltage by battery: $E_b = 36\ V,\ R_b = 40\ m\Omega$;
- in generator mode, current is limited by current density in IPM: $J_s \leq 10\ A/mm^2 \ \Rightarrow I_{lim} < 190\ A_{rms}$; and voltage by the regulation: $V_{sup} = \frac{V_{ch}}{2\sqrt{2}},\ V_{ch} = 42\ V$.

5.2 Results

We can see on figure 5 efficiencies in the torque vs. speed plan.

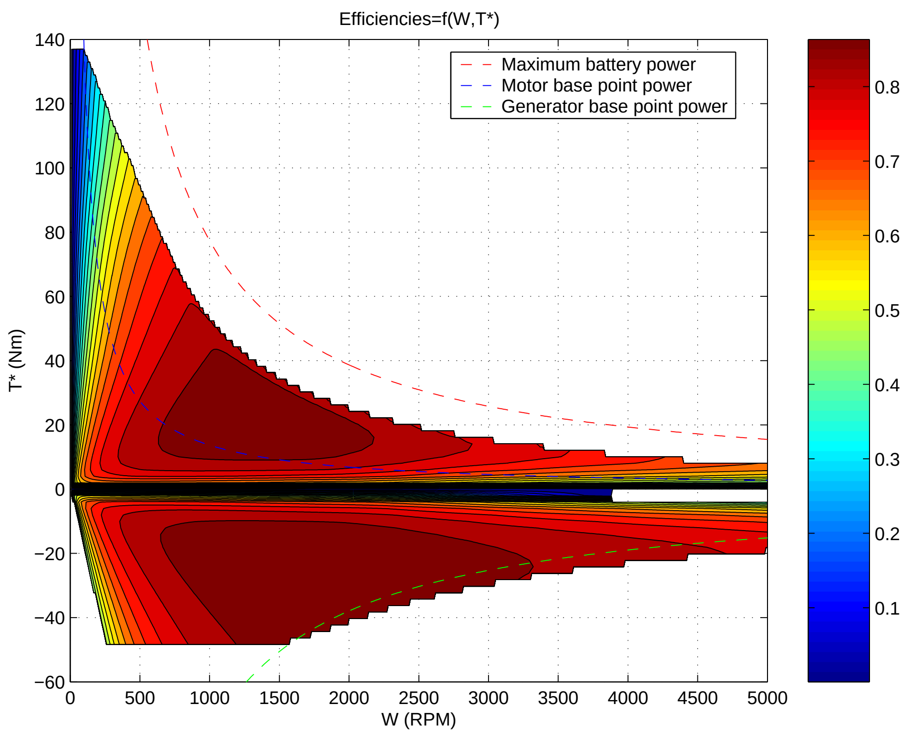

Figure 5: Efficiencies in torque vs. speed plan

Positive torques represent the starter mode, and so negative torques, the generator mode. We can see lots of differences between this two kind of operating mode:

- maximum torque is limited by the highest injectable current and the maximum electrical power. In generator, thermic conditions in steady-state limit current density;
- base speed and operating limits are directly affected by the voltage limitation. Even with our simple model of battery, the influence of the terminal voltage decreasing is very important in terms of operating range;
- in generator mode, some operating points are not accessible. For low torque or low speed, the mechanical power is not sufficient to compensate the losses (copper and iron).

6 Conclusion

This paper has examined the principle of the optimal control of interior permanent magnet synchronous machine in the starter-generator application. It has been shown that IPM particularities (permanent magnet, reluctant torque) require a precise control. The strong constraints of the ISG application, particularly the magnetic saturation and the voltage supply, have highlighted the necessity of taking into account all these non-linearities in an optimal control. This control was established by classical optimal calculations. The presented simulation results show that Interior Permanent Magnet machine is a good solution for ISG applications.

References

[1] B.J. CHALMERS, L. MUSABA, and D.F. GOSDEN. Variable-frequency synchronous motor drives for electrical vehicles. *IEEE Trans. Ind. Appl.*, 32(4):896–903, Jul./Aug. 1996.

[2] E.C. LOVELACE, T.M.. JAHNS, J.L. KIRTLEY, and J.H. LANG. An interior PM starter-alternator for automotive applications. In *Int. Conf. Electrical machines*, pages 1802–1808, Istanbul, Sep. 1998.

[3] J.R. HADJI-MINAGLOU and G. HENNEBERGER. Comparison of different motor types for electric vehicle application. *EPE Journal*, 8(3-4):46–55, Sep. 1999.

[4] G. FRIEDRICH, L. CHÉDOT, and J.M. BIEDINGER. Comparison of two optimal machine design for integrated starter-generator applications. In *Int. Conf. Electrical machines*, Aug. 2002.

[5] C. PLASSE, M. CHEMIN, G. LACAMOIRE, and E. VON WESTERHOLT. L'alterno-démarreur, du stop & go au groupe motopropulseur hybride. In *Congrès de la Société des Ingénieurs Automobile*, Versaille, Nov. 2001.

[6] C. PLASSE, A. AKEMAKOU, P. ARMIROLI, and D. SEBILLE. L'alterno-démarreur, du stop & go au groupe motopropulseur mild hybride. In *Prop'Elec*, Aix-en-Provence, Mar. 2003.

[7] N. BIANCHI, S. BOLOGNANI, and M. ZIGLIOTTO. High-performance PM synchronous motor drive for an electrical scooter. *IEEE Trans. Ind. Appl.*, 37(5):1348–1355, Sep./Oct. 2001.

[8] C.C. HWANG and Y.H. CHO. Effects of leakage flux on magnetic fields of interior permanent magnet synchronous motors. *IEEE Trans. Mag.*, 37(4):3021–3024, Jul. 2001.

[9] T.J.E. MILLER. *Brushless Permanent Magnet and Reluctant motor drive*. Oxford university press, 1989.

[10] E. KUHN. Modèle de batterie NiMH pour véhicule hybride parallèle : validation en grands signaux. In *JCGE*, Nantes, 2003.

[11] W.L. SOONG and T.J.E. MILLER. Field-weakening performance of brushless synchronous AC motor drives. *IEE Proc. - Elec. Power Appl.*, 141(6):331–340, 1994.

[12] B. MULTON, J. LUCIDARNE, and L. PRÉVOND. Analyse des possibilités de fonctionnement en régime de désexcitation des moteurs à aimants permanents. *Journal Physique III*, pages 623–640, 1995.

[13] S. MORIMOTO, Y. TAKEDA, T. HIRASA, and K. TANIGUCHI. Expansion of operating limits for permanent magnet motor by current vector control considering inverter capacity. *IEEE Trans. Ind. Appl.*, 26:866–871, Sep./Oct. 1990.

[14] G. SÉGUIER and F. NOTELET. *Electrotechnique industrielle*. Technique et documentation, 1994.

[15] Cedrat. *Analyse des dispositifs électriques, magnétiques et thermiques par la méthode des éléments finis. Notice d'utilisation générale*, Oct. 1996.

[16] The MathWorks Inc. *Optimization toolbox user's guide for use with Matlab*, 2000.